Improving the Packaging Performance of Low-Density Polyethylene With PCL/Nanocellulose/Copper(II)Oxide Barrier Layer

Nenad Đorđević[1*)], Aleksandar D. Marinković[1], Predrag Živković[1], Danijela V. Kovačević[2], Suzana Dimitrijević[1], Vanja Kokol[3], Petar S. Uskoković[1]

[1]Faculty of Technology and Metallurgy, University of Belgrade, Belgrade, Serbia
[2]Belgrade Polytechnic, Belgrade, Serbia
[3]Faculty of Mechanical Engineering, University of Maribor, Maribor

Abstract:
 A novel double layered hybrid materials, consisting of low density polyethylene (LDPE) base layer and polycaprolactone (PCL) top layer containing surface modified nanocellulose (NC) based nanocomposites in 0.5 and 2 % loadings, were studied in order to design multipurpose packaging material. NC was covalently modified with maleic anhydride (MA) to obtain NCMA, and upon co-precipitation of copper (II) oxide (CuO) on NC and NCMA surface, NC-CuO and NCMA-CuO nanocomposite materials were produced. Two drying methods, conventional and lyophilization, were applied to investigate process influences on the properties of obtained hybrid material. Oxygen transmission rate and antimicrobial activity were determined for all produced hybrid materials. PE-PCL-NCMA-CuO-L2 exhibited the highest antifungal properties, indicating contribution of MA residual group and drying conditions (liophylisation) to achievement of 97 % reduction in cell viability of C. albicans. The sample with 2 % of NCMA-CuO, PE-PCL-NCMA-CuO$_2$, demonstrated to be the most promising material regarding improvment in antibacterial and antifugal activity, as well as 16 % lower value of the oxygen transmission rate in comparison to pure LDPE.
Keywords: *Low-density polyethylene; Nanocellulose: Copper (II) oxide; Packaging.*

1. Introduction

Increased demands for the new, smart bio-based materials in food packaging, with improved performance and increased health security caused significant progress in development of innovative materials for packaging purposes [1]. Active packaging can extend shelf life, facilitate distribution of products and solve some of the environmental issues regarding pollution reduction and transition toward eco-friendly biodegradable materials. High strength, light weight, water resistance and great stability are properties that make low density polyethylene (LDPE) a good candidate material in the area of food packaging [2]. The largest disadvantages of commercially used PE as a packaging material are reflected in terms of oxygen, carbon dioxide, organic vapor and water vapor permeability. Different approaches toward modification of PE surface have proven to be effective ways for improving materials

_____

*) Corresponding author: dbrkovic@tmf.bg.ac.rs

performance and developing active and intelligent packaging. Hirvikorpi at al. used different thin film deposition techniques to obtain thin layers of Al_2O_3 on the PE surface. They showed that gas barrier properties were significantly improved once the packaging material was coated with a thin layer of Al_2O_3, regardless of employed deposition technique [3]. The advantages of organic/inorganic hybrid layered structures in producing materials with improved mechanical, antimicrobial and barrier properties have already been pointed out [4-8].

Improving surface properties of plastic packaging films trough use of bio-coatings, besides advantages in terms of low cost and biodegradability, comply with growing demands in plastic waste reduction and use of ecologically beneficial materials. Biodegradable aliphatic polyester polycaprolactone demonstrated satisfactory miscibility with wide range of polymers and PCL composites, when micro/nano scale metal oxides were used as fillers demonstrated improved antibacterial activities [9]. Application of nanosized materials in fabrication of innovative packaging is commonly related to addition of metal/metal oxide nanoparticles or different organic nanoparticles capable to serve as potential antimicrobial agents or nanosensors for the detection of food relevant analytes [10]. Polycaprolactone filled with zeolite and magnetite nanoparticles has been successfully employed as a coating layer of low density polyethylene resulting in enhanced mechanical characteristics and improved oxygen permeability of final hybrid multicomponent films [4]. Incorporation of magnetite in porous micelle structure of casein, to ensure homogeneous distribution in PCL layer, contributed to only slightly enhanced barrier (O_2 permeability) properties of final PE/PCL bilayer, despite its significantly improved mechanical and thermal features [8].

Cellulose nanocrystals (CNCs) extracted from natural cellulose sources are considered to be the most promising biodegradable nanoparticles and their inherent properties especially in terms of its high surface area, rigidity, thermal stability, anisotropic mechanical features and particularly nontoxicity provide possibilities of application in various field of science and technological innovations [11]. Introduction of functional groups trough modification of nanocellulose surface enables further adjustment of NC properties and targeted use for a specific purpose, such as antimicrobial agents [12], production of fully organic bionanocomposites [13], to enhance the hydrophobicity of paper [14], packaging applications [15], *etc*. Siqueira *et al*. demonstrated that chemical grafting of cellulose whiskers improve their compatibilization with polycaprolactone matrix [16]. A poor barrier properties of cellulose films in themselves, especially moisture barrier due to its hydrophilic nature, currently limit their extended use in packaging technology [17]. Furthermore, several studies have demonstrated that water vapor barrier properties of cellulose-based films can be enhanced by addition of inorganic particles or by coating with hydrophobic layer [18, 19]. Belbekhouche *at al*. investigated barrier properties of cellulose nanocrystals and microfibrillated cellulose (MFC) and revealed that water diffusion coefficients were higher for whiskers based film than for MFC [20]. Oxygen and water vapor barrier properties of self-standing films have been prepared from differently modified nanocellulose and nanofibrillated dicarboxylic acid cellulose film showed remarkably low oxygen permeability [21]. Several researches dealing with CNC successfully employed as a substrate for organic and inorganic nanostructures deposition or grow have been reported in literature[22, 23]. Incorporation of nanocellulose modified with magnetite nanoparticles in PCL layer enchased thermal stability and oxygen barrier properties of LDPE/PCL-nanocellulose based hybrid material [5]. However, there are no reports available on the fabrication of CNC-supported copper (II) oxide nanoparticles.

In the present work, organic–inorganic hybrid coatings consisting from PCL, nanocellulose and copper (II) oxide have been prepared in different compositions and applied to LDPE foil. First part of the study includes preparation of NC, modification of NC and fabrication of NC-CuO composites through in situ coprecipitation approach using copper (II) acetate. Subsequently, the obtained nanocellulose/copper (II) oxide composites are

incorporated in PCL layer and use as a coating layer on LDPE film.

2. Experimental procedure
2.1. Materials

All chemicals used in preparation of hybrid films, sulfuric acid, acetic acid, maleic anhydride, perchloric acid, glacial acetic acid, copper(II) acetate, sodium hydroxide and organic solvents were purchased from commercial suppliers Sigma Aldrich and Fluka, p.a. grade. Reagents and solvents were used as received. Millipore, deionized (DI) water (18 MΩ cm resistivity) was used for sample washing and solution preparation. Polycaprolactone (PCL), average molecular weight of ~45000, was purchased from Sigma-Aldrich. Polyethylene foil LG SP 311 (LDPE) was supplied by Macchi (three layer folio 28/44/28 %).

2.2. Preparation procedures
2.2.1. Preparation of nanocellulose (NC) and modification with maleic anhydride (NCMA)

Nanocellulose nanocrystals (NC) were prepared by acid hydrolysis of commercially available cellulose according to established procedure [24]. Afterwards, NC was modified by esterification with maleic anhydride according to slightly modified literature method [25]. In order to change solvent for the chemical modification of nanocellulose, the obtained cellulose nanoparticles were washed with acetic acid. The sample of 20 g nanocellulose was prepared for modification with maleic anhydride by alternately washing and centrifugating with acetic acid three times in order to exchange of solvent. The sample was placed in a stoppered glass bottle containing a mixture of 160 ml of acetic acid and 200 ml of toluene and homogenized on ultrasonic bath (Bandelin electronic, Berlin, Germany, power of 120 W and frequency of 35 kHz) sonicated for 1 min. After homogenization, 0.8 ml of 60 % perchloric acid was added, reaction mixture was sonificated for 1 min, and then, 0.5 g of maleic .anhydride was added. The mixture was allowed to stand for 1 h at room temperature. After the reaction the NC sample was thoroughly washed and centrifugated with toluene, methanol and dichloromethane, respectively.

2.2.2. Preparation of NC/copper oxide composites

Copper oxide nanocellulose composites were prepared by hydrolysis of copper(II) acetate in the presence of sodium hydroxide according to slightly modified literature procedure [26]. 2.0 g of appropriate nanocellulose sample (NC or NCMA) was dispersed in 300 ml of water. 0.02 M of $[Cu(CH_3COO)_2 \cdot H_2O]$ was dissolved in a prepared mixture and 1 ml of glacial acetic acid was added in order to prevent hydrolyzation of Cu^{2+} ions. 0.05 M of NaOH was used as reducing agent. The solution was heated at 60 °C with stirring during the next 4 hours. The suspension turned dark blue in color and pH of the initial solution increased from 12.27 to 12.89. The precipitate was centrifuged and washed several times with DI water and ethanol. The resulting particles were dried in two different manners. The first samples were dried under vacuum at 80 °C for 6h to obtain black powder (NC-CuO and NCMA-CuO) and the second were exposed by freeze-drying (lyophilisation) in order to obtain samples NC-CuO-L and NCMA-CuO-L [26].
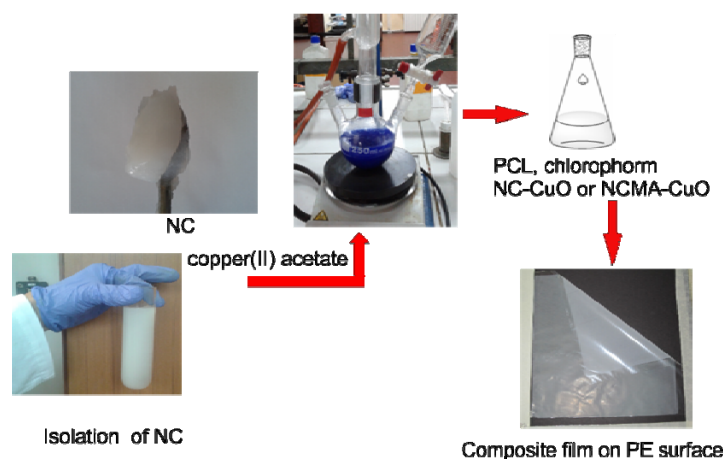
Fig. 1. Preparation procedure of PCL composite film on PE surface.

Tab. I Composition of PE hybrid samples coated with PCL/nanocellulose/CuO films.

	Samples	Filler in PCL composite layer	%
1	PE	/	0
2	PE-PCL	/	0
3	PE-PCL-NC0.5	NC	0.5
4	PE-PCL-NC2	NC	2
5	PE-PCL-NCMA0.5	NCMA	0.5
6	PE-PCL-NCMA2	NCMA	2
7	PE-PCL-NC-CuO0.5	NC-CuO	0.5
8	PE-PCL-NC-CuO2	NC-CuO	2
9	PE-PCL-NCMA-CuO0.5	NCMA-CuO	0.5
10	PE-PCL-NCMA-CuO2	NCMA-CuO	2
11	PE-PCL-NC-CuO-L0.5	NC-CuO-L	0.5
12	PE-PCL-NC-CuO-L2	NC-CuO-L	2
13	PE-PCL-NCMA-CuO-L0.5	NCMA-CuO-L	0.5
14	PE-PCL-NCMA-CuO-L2	NCMA-CuO-L	2

2.2.3. Preparation of composite film on polyethylene surface

Polycaprolactone (PCL) solution of 10 wt.% was prepared by dissolving PCL pellets in chloroform (Fig. 1). After the PCL was dissolved by using combination of both mixing and ultrasound treatment, the solutions were used for preparation of PCL based composite dispersion. PE/nanocellulose composite hybrid structures were prepared by extruding PE, and then coating it with a thin film of differently modified nanocellulose. Polycaprolactone (PCL) was used as a binder in order to provide uniform film formation on polyethylene surface. Composition of PE hybrid films is presented in Tab. I.

2.3. Characterization of unmodified and modified NC and NC/CuO composites

X-ray diffraction (XRD) data were obtained using a BRUKER D8 ADVANCE with Vario 1 focusing primary monochromator (Cu $k_{\alpha 1}$ radiation, $\lambda = 1.54059$ Å). XRD patterns were obtained over the Bragg angle (2θ) range of 10-90°.

Raman spectra were collected with a XploRA Raman spectrometer from Horiba Jobin Yvon. The system employed laser at 532 nm (maximum output power 20-25 mW).

The thermal properties of nanocellulose/copper oxide samples were analyzed using a TA Instruments Q600. Dry samples were heated under nitrogen atmosphere, between ambient temperature and 700 °C, at heating rate of 20 °C/min.

Scanning electron microscopy (FEG-SEM) was performed with a field emission gun TESCAN MIRA3 XMU electron microscope for recording the images of the surfaces of NC and NC composites.

2.4. Determination of Oxygen Transmission Rate (OTR) of double layered hybrid material

The samples were conditioned at 20±2 °C and 60±5 % RH for 24 hours before measuring the OTR. OTR through film samples is determined at pre-defined conditions (e.g. 23±2 °C and 50±5 % RH) using an oxygen transmission rate test machine with the use of a Perme OX2/230 (Labthink Instruments Co., Ltd.). Film thickness is measured with the electronic digital caliper before the testing and inputted to the computer program WinPerme OX2-230 W3-330(En). The OTR is measured after the film had been placed in a cell and the oxygen flow introduced on one side of the film. The OTR (ml m^{-2} day^{-1}) is calculated from the mean OTR multiplied by the film thickness (mm) and divided by the oxygen gradient within the cell of the testing machine (1 kgf cm^{-2}). Three independent determinations are carried out for each film sample and the mean of these three values is given as the final result.

2.5. Determination of antibacterial properties of double layered hybrid material

Antibacterial properties of prepared LDPE based hybrid films was exanimated according to ISO 22196:2007 method with some modification. Briefly, the film samples (25x25 mm) are placed into a separate sterile Petri dish with the test surface uppermost. A quantity of 50 μL of the test inoculum was placed onto the test surface from appropriate saline solution and covered with a UV sterilized parafilm that is gently pressed down so that the test inoculum spreads to the edges. The Petri dish was covered and incubated for 24 h at 37 °C. For recovery of bacteria, 10 ml of neutralizer solution was added with gently shaking and 1 mL aliquot was used for viable cells determination. The percentage of reduction of the microbial cells (R, %) was calculated using the following equation (1):

$$R(\%) = \frac{CFU_{init} - CFU_{samo}}{CFU_{init}} \cdot 100 \qquad (1)$$

where CFU_{init} and CFU_{samp} are the numbers of colony forming units per milliliter for the initial number and the sample, respectively. All experiments were performed in triplicates and the results are shown as mean values.

3. Results and Discussion
3.1. XRD analysis

The crystal structure of the NC/CuO composites is determined from the powder X-ray diffraction patterns shown on Fig. 2. The XRD diffractograms of composites containing CuO nanoparticles exhibited two distinct peaks of nearly equal intensities at diffraction angles of 35.6° and 38.5°.
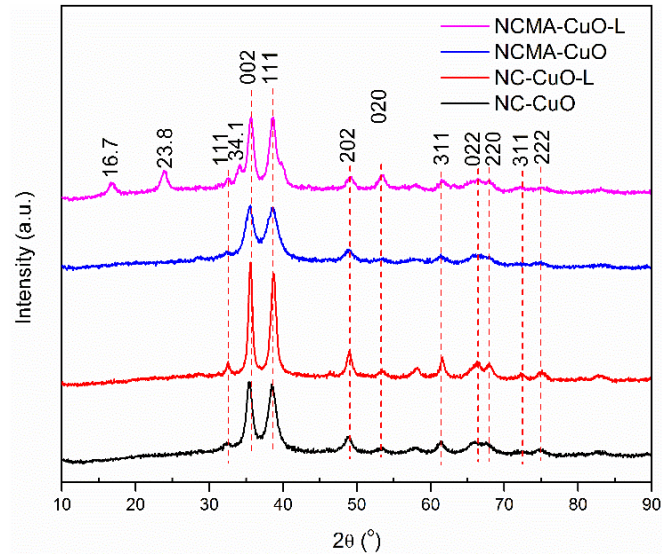
Fig. 2. XRD diffractograms of NC-CuO, NC-MA-CuO, NC-CuO-L
and NC-MA-CuO-L.

The atomic planes were undoubtedly assigned on following Fig. and it can be stated the presence of only pure monoclinic phase of CuO (JCPDS No. 05-0661) [26-27]. The signals of some impurities, such as Cu_2O or $Cu(OH)_2$ were not observed. Moreover, the signals of nanocellulose are not present in the diffractograms of NC-CuO, NCMA-CuO and NC-CuO-L, while some of the NC signals are found in a diffraction pattern of the sample NCMA-CuO-L. The peak corresponding to [200] plane of cellulose is shifted toward higher value of Bragg's angle (from 22° to 23.7°), while [004] atomic plane of cellulose I is shifted to a lower value (34.1°) The differences between CuO nanostructures (flower or sheets) is not possible to be driven from the XRD diffraction patterns [28].

3.2. Raman analysis

Raman analysis was employed in order to detailed investigate structural composition of NC, NCMA and nanocellulose/copper oxide composites.
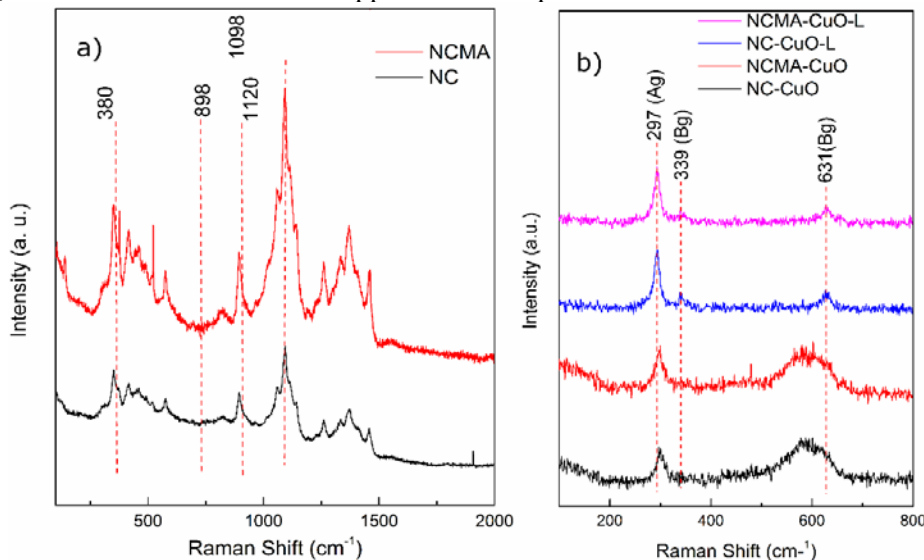

Fig. 3. Raman spectra of NC, NCMA and nanocellulose/copper oxide composite samples.

Raman spectra of NC and NCMA were presented on Fig. 3a. The Raman signals attributed to NC groups have been observed. Signal at 380 cm^{-1} is assigned to hydroxyl groups, while the peak at 898 cm^{-1} is attributed to C−OH bending at C-6 [11]. The bands located in the range of 250–600 cm^{-1} are due to skeletal-bending modes CCC, COC, OCC and skeletal stretching modes of CC and CO [29, 30]. Signal at 1098 cm^{-1} is due to C−O−C ring stretching modes and the β-1,4 glycosidic linkage (C–O–C) stretching modes in cellulose chains [30-32]. The band centered at 1120 cm^{-1} corresponds to C−O−C bending in nanocellulose structure [11]. The difference from NC and NCMA is reflected only in intensity of Raman signals.

Semiconducting features of copper oxide determine its crystallization in monoclinic structure and 12 vibrational modes normal: Γ́= 4Au + 5Bu + Ag+ 2Bg are identified for CuO [33]. Three of those are acoustic modes (Au + 2Bu), six are infrared active modes (3Au + 3Bg) and three Raman active optical phonons. The displacement of oxygen atom in CuO symmetric structure affects only three Raman active modes (Ag + 2Bg) [33], [34]. Copper atoms have no impact on Raman active optical phonons. The three active peaks at 297 (Ag), 339 (Bg) and 631(Bg) cm^{-1} in Raman spectra of all composite sample containing CuO are present (Fig. 4b). Results of Raman analysis undoubtedly confirmed single phase monoclinic CuO nanostructures. The Raman peaks position in the cases of NC-CuO and NCMA-CuO is slightly downshifted and signals are broader comparing to the samples exposed by freeze-drying (lyophilisation). The difference in the Raman spectra of samples dried under vacuum and by freeze-drying is expected, indicating changes in CuO morphology, considering that Raman signal position depend on the preparation method, geometry and crystal structure.

3.3. TG analysis

Thermal gravimetric analysis was used to investigate thermal properties of prepared nanocellulose/copper(II) oxide samples in order to determine residual copper oxide i.e. quantitative determination of CuO loading.
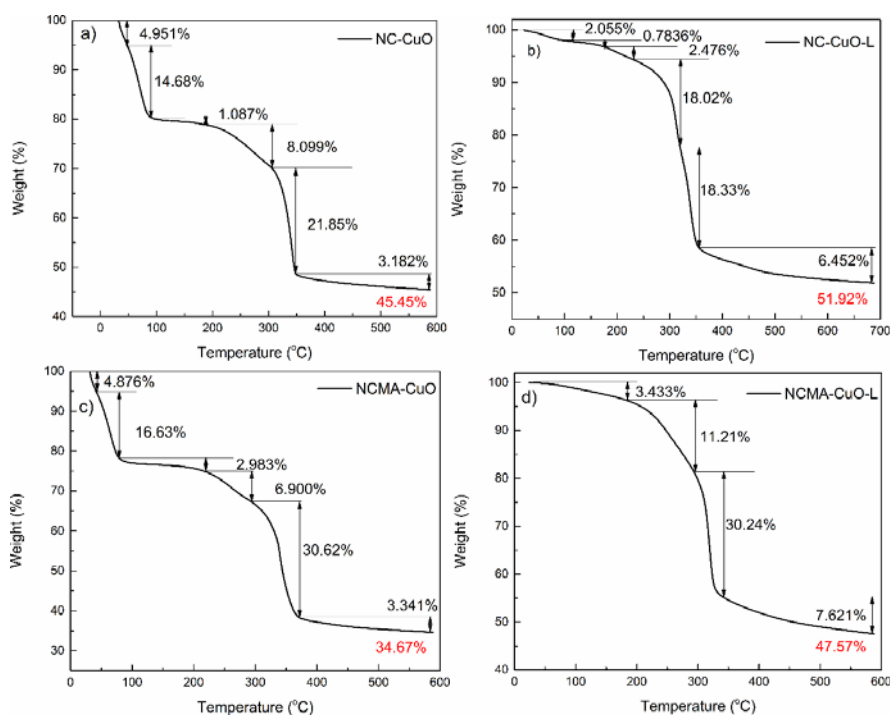

Fig. 4. Thermograms of NC-CuO, NC-CuO-L, NCMA-CuO and NCMA-CuO-L.

Thermal gravimetric analysis was used to investigate thermal properties of prepared nanocellulose/copper (II) oxide samples and in order to determine residual copper oxide i.e. quantitative determination of CuO loading. TG curves are presented on Fig. 4. The significant increase in thermal stability of all nanocellulose/copper (II) oxide samples compared to NC and NCMA is observed. Determination of CuO loadings indicates higher concentration of metal oxides on the top of unmodified NC substrate. Hydrophobic MA residue did not promote precipitations of CuO on modified NC surface. The drying procedure in both cases had an important influence in the amount of adsorbed groups. The conventional drying procedure (vacuum oven on 80 °C for 6h) did not completely removed adsorbed groups (water, moister, oxygen groups) from the CuO surface, while lyophilisation procedure showed the opposite effect. The smaller quantities of adsorbed group when lyophilisation procedure was used resulted in a less weight loss in the cases of both samples.

3.4. SEM

SEM micrographs of NC and NCMA presented on Fig. 5 a) - b) revealed the significant changes in the morphology of those two samples.
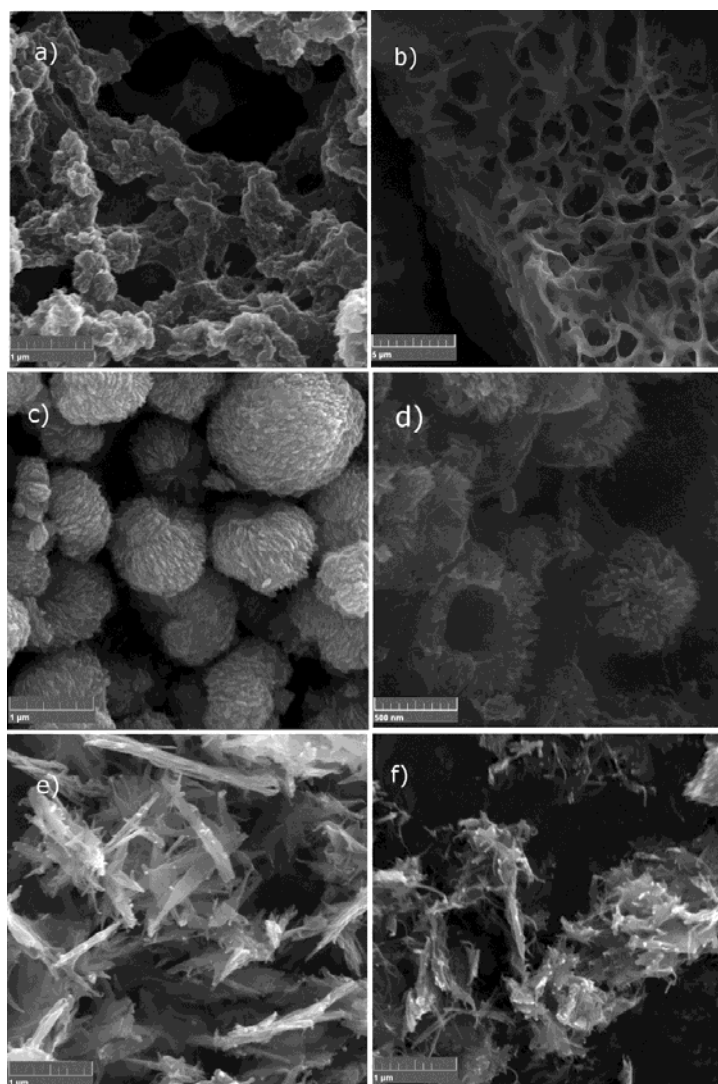

Fig. 5. SEM micrographs of a) NC, b) NCMA c) NC-CuO nanoflower, d) NC-MA-CuO, e) NC-CuO-L nanoleaf, f) NC-MA-CuO-L nanoleaf.

NCMA showed more uniform and interconnected porous structure, while the NC samples appear like interlinked bundles different in the size and shape. SEM micrographs of NC/copper oxide composites, shown on Fig. 5 c) - f) provide inside on morphological changes of the final products. It can be pointed out that NC modification and drying procedure crucially affects and defines CuO nanostructure in the composite material. The precipitation of copper oxide on unmodified NC (Fig. 5c) results in a well-defined characteristic quasi-spherical microarchitectures [26]. A solid microspheres had an average diameter of around ~ 1μm. Although FT–IR and XRD results indicate that modification of NC with maleic acid anhydride does not affect NC structure to a greater extent, it crucially determines form of CuO and results in creation of less defined hollow quasi-spherical microstructure having similar diameter (~ 1μm).

It can be concluded that nanocellulose particles play important role as stabilizing agent, enable to coordinate metal ions in different growth pathway leading to the formation of nanostructures of different morphology. Hence, the unmodified NC particles serve as a nuclei for creation of the quasi-spherical microarchitectures, while the MA residue contributes to the creation of less defined hollow formation of CuO particles coated on NCMA surface.

The lyophilization procedure causes a considerable changes in a final morphology of both samples. Fig. 5 e) illustrates the formation of the nanoleaves and complete degradation of the initial quasi-spherical microarchitectures of NC-CuO and NCMA-CuO upon lyophilization was performed. The structure of NC-MA-CuO-L is similar to the structure observed in the case of NC-CuO-L, the difference is evident in terms of the nanoleaves size. In fact, during the lyophilisation process, the MA residue on the NC surface favors formation of thinner nanoleaves, smaller in size and more agglomerated. Raman analysis of the nanocellulose/copper oxide composites revealed slight differences in peak position and shape depending on the drying procedure, confirm that resulting CuO nanoparticles had different morphology which is in accordance with SEM findings. The size and shape of the co-precipitated CuO nanoparticles were found to be strongly dominated by the nature of substrate (NC or NC with MA residue) and drying conditions.

3.5. Antimicrobial properties

Antimicrobial studies are carried out using *Escherichia Coli* (ATCC 25922*)* as model of Gram-negative bacteria, *Staphylococcus Aureus* (ATCC 25923*)* as model of Gram-positive bacteria and fungus *Candida Albicans* (ATCC 10259). Quantitative antibacterial and antifungal studies of different LDPE covered PCL/NC based composite films are performed by incubating the hybrid films with *E. coli, C. albicans* and *S. aureus* in suspensions with starting concentrations of 4.5×10^5, 3.2×10^5 and 3.7×10^5 CFU/ml respectively. The percentages of cells reduction (*R*, %) of *E. coli, S. aureus* and *C. albicans* after 24 h are shown on Fig. 6. All films containing copper oxide nanoparticles exhibit a significantly antibacterial efficacy against *E. coli,* although slightly better results demonstrated film with NC/copper oxide composites dried on conventional way.

In the case of *C. albicans,* the samples containing NC and NCMA exhibit negligible antifungal activity while precipitation of CuO on NC and NCMA surface exceptionally increased reduction in cell viability of *C. albicans* and highest antifungal activity reached value of 97 % for the hybrid film PE-PCL-NCMA-CuO-L2. It seems that drying procedure - liophylisation and MA residue, i.e. the morphology of CuO nanoparticles and the distribution on NCMA substrate in the nanocellulose/CuO composites, enabled successful elimination and inhibited microbial growth of *C. albicans* in the final hybrid double-layered film.

The prepared hybrid films exhibited fewer antibacterial properties against *S. aureus*, compared to *E. coli* and initial number of microbial colonies decreased distinctly only in the case of PE-PCL-NCMA-CuO2 (77.8 %). This study revealed crucial impact of CuO morphology on particular antimicrobial activity of manufactured films. The specific size and

shape of CuO nanoparticles and their assembling can result in well-defined antimicrobial activity and provide protection directed either against individual bacterial/fungal species or a wide range of pathogenic microorganisms.
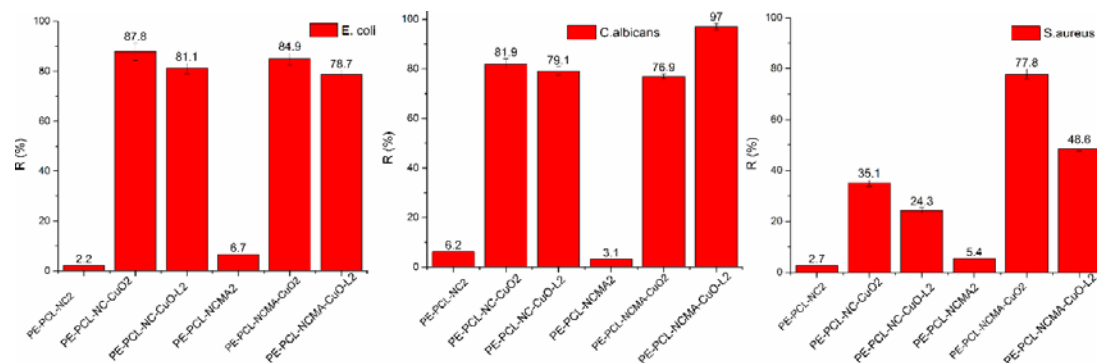

Fig. 6. The percentages of cells reduction (*R*, %) of *E. coli, S. aureus* and *C. albicans.*

Incorporation of 2 wt% of NC-CuO nanoflowers in PCL coatings (sample PE-PCL-NC-CuO2) causes considerable antibacterial (reduction in cell viability of *E. coli* reached 87.8 %) and antifungal properties (reduction in cell viability of *C. albicans* is 81.9 %). Also sample PE-PCL-NCMA-CuO-L2 demonstrated excellent antifungal (inhibition of 97 %) and moderate antibacterial properties are observed.

3.6. Barrier properties

Values of oxygen transmission rate (OTR) of LDPE and LDPE covered PCL/NC based composite films are presented in Tab. II. All investigated multicomponent films demonstrated lower oxygen transmission rate value compared to both PE and PE-PCL samples, indicating contribution of NC, NCMA and copper-oxide inside polycaprolactone matrix to improved barrier properties with respect to oxygen.

Tab. II Values of oxygen transmission rate.

SAMPLE	OTR (cm^3/m^{2}d)
PE	5026.537
PE-PCL	4702.589
PE-PCL-NC2	4138.668
PE-PCL-NCMA2	3569.029
PE-PCL-NC-CuO2	4302.573
PE-PCL-NCMA-CuO2	4231.178
PE-PCL-NC-CuO-L2	4478.255
PE-PCL-NCMA-CuO-L2	4377.753

The group of authors showed that presence of magnetite incorporated in casein in PCL layer had almost negligible impact on oxygen barrier properties of final PE/PCL films [8], while the PCL layer having higher content of magnetite in zeolite resulted in significant improvements in oxygen barrier performance of PE/PCL bilayer [7]. The sample containing NCMA reached the higest decrease in oxygen transmission rate. Both samples containing fillers dried by liophylisation showed higher values of oxygen transmission rate compared to corresponding films containing NC-CuO and NCMA-CuO dried in conventional conditions.

Even though sample PE-PCL-NCMA2 showed the higest decrease in oxygen transmission rate (almost 30% compared to the initial material) its poor antimicrobial properies restrict the potentional application of this sample as a packaging material. The PE-PCL-NCMA-CuO2 is bilayer multicomponent film with the best packaging performance, considering its good antimicrobial activity aganst fungi, Gram-negative and Gram-positive bacterias and improved barrier performance regarding oxygen transmission rate.

4. Conclusion

Development of a double layered multicomponent hybrid films composed of LDPE coated with PCL-NC based composite layer has been conducted. In order to improve barrier and antimicrobial properties of LDPE, modified and unmodified NC-CuO and NCMA-CuO composites, respectively, were used as a filler for PCL based composite layer. Detailed structural, morphological and thermal characterization of nanocomposites has been performed. Hybrid packaging material PE-PCL-(NC or NCMA)-CuO, at 0.5 % and 2 % of NC-CuO or NCMA-CuO loading, showed improved oxygen transmission rate, as well as antimicrobial performance. Incorporation of 2 wt% of NC-CuO nanoflowers in PCL coatings, sample PE-PCL-NC-CuO2, causes 87.8 % reduction in cell viability of *E. coli* and 81.9 % reduction in cell viability of *C. albicans*. Also, sample PE-PCL-NCMA-CuO-L2 showed excellent antifungal activity. Liophylisation do not contribute to improvement of barrier properties. Sample PE-PCL-NCMA2 showed the higest decrease in OTR (about 30 %), while undesirable poor antimicrobial properies restrict the potentional application as a packaging material. The PE-PCL-NCMA-CuO2 is bilayer multicomponent film with the best packaging performance, considering its good antimicrobial activity against fungi and bacteria, while improved barrier performance, regarding lower OTR value with respect to LDPE, was also obtained.

Acknowledgement

5. References

1. D. Dainelli, N. Gontard, D. Spyropoulos, E. Zondervan-van den Beuken, P. Tobback, Trends Food Sci. Technol., 19 (2008) S103.
2. A. P. Siročić, A. Rešček, M. Ščetar, L. K. Krehula, Z. Hrnjak-Murgić, Polym. Bull., 71 (2014) 705.
3. T. Hirvikorpi, M. Vähä-Nissi, A. Harlin, M. Karppinen, Thin Solid Films, 518, (2010) 5463.
4. A. Rešček, Z. Katančić, L. K. Krehula, M. Ščetar, Z. Hrnjak-Murgić, K. Galić, Adv. Polym. Technol., (2016) in press DOI: 10.1002/adv.21727.
5. N. Djordjević, A. Marinković, J. Nikolić, Š. Drmanić, M. Rancić, D. Brković, P. Uskoković, J. Serbian Chem. Soc., 81 (2016) 589.
6. R. Shemesh, M. Krepker, D. Goldman, Y. Danin-Poleg, Polym. Adv. Technol., 26, (2015) 110.
7. A. Rešček, L. Kratofil Krehula, Z. Katančić, Z. Hrnjak-Murgić, Croat. Chem. Acta, 88 (2015) 461.
8. A. Rešček, M. Ščetar, Z. Hrnjak-Murgić, N. Dimitrov, K. Galić, *Polym. Plast.*

Technol. Eng., 55 (2016) 1450.

9. M. Shoja, K. Shameli, M. B. Ahmad, K. Kalantari, Dig. J. Nanomater. Biostructures, 10 (2015) 169.
10. T. V. Duncan, J. Colloid Interface Sci., 363 (2011).
11. P. Dhar, A. Kumar, V. Katiyr, ACS Appl. Mater. Interfaces, 8, (2016) 18393.
12. A. Jebali, S. Hekmatimoghaddam, A. Behzadi, I. Rezapor, B. H. Mohammadi, T. Jasemizad, S. A. Yasini, M. Javadzadeh, A. Amiri, M. Soltani, Z. Rezaei, N. Sedighi, M. Seyfi, M. Rezaei, M. Sayadi, Cellulose, 20 (2013) 2897.
13. E. Espino-Pérez, J. Bras, V. Ducruet, A. Guinault, A. Dufresne, S. Domenek, Eur. Polym. J., 49 (2013) 3144.
14. W. Zhang, R. K. Johnson, Z. Lin, C. Chandoha-Lee, A. Zink-Sharp, S. Renneckar, Cellulose, 20 (2013) 2935.
15. G. Rodionova, M. Lenes, O. Eriksen, O. Gregersen, Cellulose, 18, (2011) 127.
16. G. Siqueira, J. Bras, A. Dufresne, Biomacromolecules, 10 (2009) 425.
17. A. Arora, G. W. Padua, J. Food Sci., 75 (2010) 43.
18. K. L. Spence, R. A. Venditti, O. J. Rojas, J. J. Pawlak, M. A. Hubbe, BioResources, 6 (2011) 4370.
19. S. Ummartyotin, J. Juntaro, M. Sain, H. Manuspiya, Ind. Crops Prod., 35 (2012) 92.
20. S. Belbekhouche, J. Bras, G. Siqueira, C. Chappey, L. Lebrun, B. Khelifi, S. Marais, A. Dufresne, Carbohydr. Polym., 83 (2011) 1740.
21. J. A. Sirvio, A. Kolehmainen, M. Visanko, H. Liimatainen, J. Niinima, O. Hormi, Appl. Mater. Interfaces, 6 (2014) 14384.
22. C. M. Cirtiu, A. F. Dunlop-Brière, A. Moores, Green Chem., 13 (2011) 288.
23. Y. Shin G. J. Exarhos, Mater. Lett., 61 (2007) 2594.
24. D. Bondeson, A. Mathew, K. Oksman, Cellulose, 13 (2006) 171.
25. D. Y. Kim, Y. Nishiyama, S. Kuga, Cellulose, 9 (2002) 361.
26. S. Anandan, G. J. Lee, J. J. Wu, Ultrason. Sonochem., 19 (2012) 682.
27. C. Deng, H. Hu, X. Ge, C. Han, D. Zhao, G. Shao, Ultrason. Sonochem. 18 (2011) 932.
28. C. Yang, F. Xiao, J. Wang, X. Su, Sensors Actuators B Chem., 207 (2015) 177.
29. A. E. Lewandowska, S. J. Eichhorn, J. Raman Spectrosc., 47 (2016) 1337.
30. H. Wiley, R. H. Atua, Carbohydr. Res., 160 (1987) 113.
31. A. E. Lewandowska, C. Soutis, L. Savage, S. J. Eichhorn, Compos. Sci. Technol., 116 (2015) 50.
32. N. Gierlinger, M. Schwanninger, A. Reinecke, I. Burgert, Biomacromolecules, 7 (2006) 2077.
33. J. C. Irwin, J. Chrzanowski, T. Wei, Phys. C, 166 (1990) 456.
34. M. A. Dar, Q. Ahsanulhaq, Y. S. Kim, J. M. Sohn, W. B. Kim, H. S. Shin, Appl. Surf. Sci., 255 (2009) 6279.

Садржај: *У овом раду су синтетисани двослојни, хибридни, амбалажни материјали који се састоје од слоја полиетилена мале густине (LDPE) и слоја поликапролактона (PCL) и коме се налази 0,5 и 2 мас.% композита на бази наноцелулозе (NC) и бакар оксида. Наноцелулоза је најпре ковалентно модификована анхидридом малеинске киселине (NCMA), а затим је на површину наноцелулозе и модификоване наноцелулозе (NC и NCMA), извршено таложење честица бакар (II) оксида (CuO) и добијени нанокомпозитни материјали NC-CuO и NCMA-CuO. Примењене су две различите методе сушења нанокомпозитних узорака и то конвенционално сушење и лиофилизација како би се испитао утицај ових процеса на својства хибридних материјала. Одређена је пропустљивост свих хибридних филмова на кисеник, као и њихова антимикробна активност. Узорак PE-PCL-NCMA-CuO-L2 је показао најбољу*

активност против гљивица, чак 97 % редукције C. albicans указујући тиме на допринос како анхидрида малеинске киселине, тако и сушења композитних узорака процесом лиофилизације. Узорак са 2 % NCMA-CuO, PE-PCL-NCMA-CuO2 се показао као потенцијално најбољи амбалажни материјал јер је поред добрих антибакеријских и антигљивичних својстава, уочено и побољшање баријерних својстава. Пропустљивост на кисеоник је код овог узорка опала за 16 % у поређењу са чистим филмом LDPE.
Кључне речи: полиетилен мале густине, наноцелулоза, бакар (II) оксид, амбалажни материјал.